Paper:

Numerical Simulations of Volcanic Ash Plume Dispersal from Kelud Volcano in Indonesia on February 13, 2014

Hiroshi L. Tanaka*, **Masato Iguchi****, **and Setsuya Nakada*****

*Center for Computational Sciences, University of Tsukuba
Tsukuba 305-8577, Japan
E-mail: tanaka@ccs.tsukuba.ac.jp
**Sakurajima Volcano Research Center, Disaster Prevention Research Institute, Kyoto University
Kagoshima 891-1419, Japan
***Earthquake Research Institute, University of Tokyo
Tokyo 113-0032, Japan
[Received September 1, 2015; accepted January 3, 2016]

In order to evaluate airborne ash densities, a real-time volcanic ash dispersion model, PUFF, is applied to the February 13, 2014 eruption of Kelud volcano in Indonesia. The emission rate of the ash mass from the vent is estimated based on the empirical formulae tested at Sakurajima volcano using ground deformation and seismic monitoring data.
According to the result of the PUFF model simulation, the circular shape of the anvil ash cloud 17 km in height extends during the first two hours over a radius of 200 km from the volcano. The core region within 50 km of the volcano shows an airborne ash density of 1000 mg/m^3. Three hours after the initial eruption, the area with 100 mg/m^3 extends 300 km to the west, covering Yogyakarta Airport. Due to low-level winds, Surabaya Airport to the northeast also becomes part of the area with 100 mg/m^3. The result of the ash plume dispersal 7 hours into the eruption indicates that the entire island of Java is in the danger zone for commercial airliners, as ash exceeds 10 mg/m^3. Although satellite images show that the ash plume is located only in the southern half of western Java, the simulation results quantitatively indicate much wider extents of the aircraft danger zone.

Keywords: PUFF model, Kelud volcano, aviation safety, airborne ash density, ash dispersion

1. Introduction

Volcanic ash floating and traveling in the air far from the erupting volcano is a great concern to aviation safety. The first major incident caused by volcanic ash occurred in June 1982. British Airways Flight 9, a B-747, was flying over Galunggung, a volcano in Indonesia. All four engines stopped for 12 minutes due to the intake of dense floating ash from the volcano. However, the cause of the engine failure was not immediately clear to either the crew or air traffic control. The aircraft was diverted to Jakarta and, thanks to the recovery of some of its engines, landed safely. When a commercial airliner encounters an airborne ash plume, the damage is an estimated 1 million US dollars for the replacement of the jet engines, and 1 billion US dollars if the aircraft crashes, the worst case scenario.

The first well known report of a serious encounter with an airborne ash plume was an incident involving a KLM jumbo jet approaching Anchorage International Airport from Europe in December 1989. At that time, the aircraft was flying over Mt. McKinley, Mt. Redoubt was erupting and ejecting large amounts of ash into upper troposphere, and the ash had traveled 300 km northeast from the volcano. All four engines stopped due to the intake of volcanic ash, which melted and jammed in the engines. The aircraft stalled and lost power, dropping to 10000 feet above the ground (Hobbs et al., 1991; Casadevall, 1994). It was quite fortunate that jammed ash cooled and passed out of the engines, allowing it to recover.

After this incident, the International Civil Aviation Organization (ICAO) established Volcanic Ash Advisory Centers (VAAC) in 9 sectors around the world. The Tokyo VAAC, established in 1997, is one of the 9 VAACs (see Onodera, 1997). The Darwin VAAC covers the area of Oceania including Indonesia. However, similar incidents involving commercial airliners encountering volcanic ash have occurred many times along Oceanian routes. These incidents have been caused by ash from the Pinatubo eruption in 1991 as well as from a number of other active volcanoes, including Galunggung, Guntur, Kelud, Merapi, and Semeru in Indonesia.

Kelud volcano (1.731 km asl) in Indonesia was the scene of a major Plinian eruption at 15:50 UTC (22:50 local time) and again at 16:30 UTC (23:30 local time) on February 13, 2014. The umbrella-shaped ash plume reached well into the stratosphere. According to GMS satellite monitoring (see **Fig. 1**), the top of the plume, reaching nearly 17 km in height, spread nearly evenly around the volcano. The circular anvil cloud reached a radius of about 100 km during the first hour, and it expanded to 200 km two hours after the initial eruption owing to the explosive momentum of the initial velocity and the diverg-

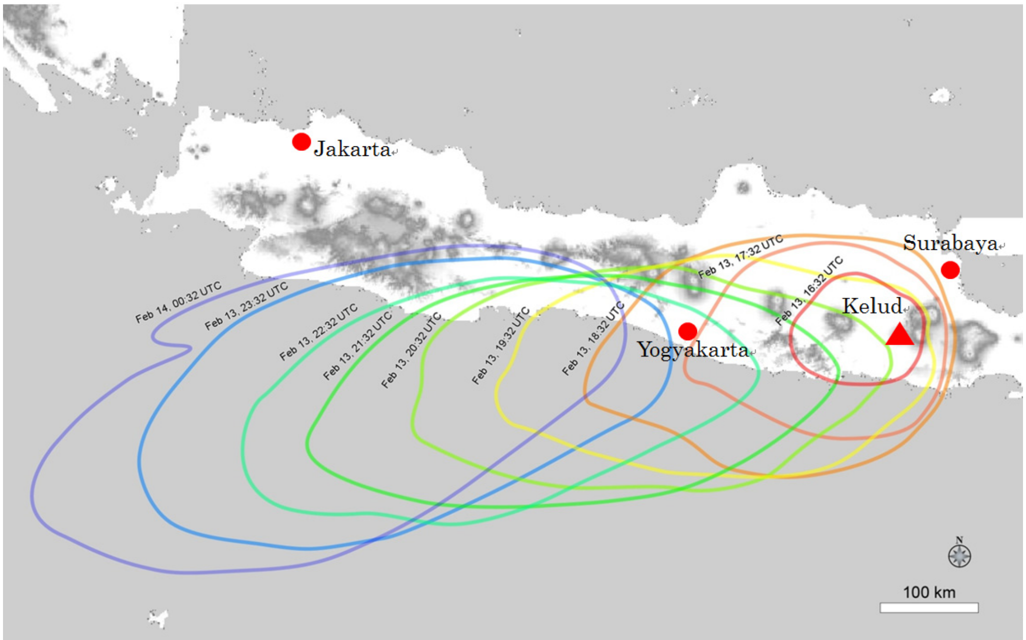

Fig. 1. Eruption plume of Kelud volcano in Indonesia on February 13, 2014. The lines indicate the area and dispersal for each hour from 16:32 UTC (red circle) to 24:32 UTC. (Figure by F. Maeno and others, under preparation).

ing mass flux from the volcano. The circular shape of the plume top started to drift westward across the island of Java holding the same radius at three hours after the eruption, and it continued moving westward with a gradual spread due to diffusive mixing. Nine hours into the eruption, the center of the plume top had drifted about 600 km westward over the Indian Ocean. By that time, the plume top had a radius of 300 km. The estimated ash fallout was 8 cm thick over an area with a radius of 25 km from the volcano. The depth decreased to 1 cm at 280 km west near Yogyakarta and at 140 km northeast near Surabaya. In fact, ash fallout 50 cm thick was reported at Ngantang in Malang. A thickness of 2 cm was reported at the airports of Surabaya, Yogyakarta, and Solo. The airports closed and 150 domestic flights were canceled on February 14. Slight fallout was also reported at Borobudur Temple and Bandung in West Java. Four people died in the eruption, and 200,000 people within a 10 km area around the volcano were evacuated by February 15, according to the official report by the local newspaper February 17 in Jakarta.

In order to reduce the hazard to the aviation industry, the VAAC has developed a number of ash plume dispersion models. Refer to Leadbetter et al. (2010) for the recent NAME model applied for the Eyjafjallajokull eruption in April 2010, Thomas and Watson (2010) for the application of satellite monitoring, Folch (2012) for the review of the tephra transport and dispersal model, and comprehensive reviews by Prata (2009) and Onodera (2013) for the volcanic hazard and aviation safety. Previously, a 3D turbulent diffusion model was developed by Armienti and Macedonio (1988) using observed upper air wind data and was applied to the Plinian eruption of Mt. St. Helens in 1980. Glaze and Self (1991) constructed a turbulent diffusion model considering the vertical wind shear and applied it to the Usu volcano eruption in 1977 to explore the distribution of ash fall. Hurst and Turner (1999) developed a 3D turbulent diffusion model, ASHFALL, to predict volcanic ash fall for operational use. Heffter and Stunder (1993) developed a transport dispersion model, Volcanic Ash Forecast Transport and Dispersion (VAFTAD), to predict the transport and dispersion of volcanic ash after an eruption. The Tokyo VAAC operates the Lagrangian and Eulerian models to forecast the position of volcanic ash clouds (Tokyo Aviation Weather Service Center, 2001).

In addition to these activities, Tanaka (1994) has developed a real-time volcanic ash plume tracking model, the PUFF model, at the Geophysical Institute of the University of Alaska Fairbanks. The PUFF model was applied to volcanos in the northeastern Pacific Rim by Searcy et al. (1998). The PUFF model has been operational under the Alaska Volcano Observatory since the eruption of Redoubt volcano in 1990 (Tanaka, 1991; Kienle et al., 1991; Dean et al., 1993). Since then, it has also been used by the US Geological Survey, US National Weather Service, Japan Airlines, Japan Weather Association, and the University of Tsukuba, Japan. In this Lagrangian model, forecast wind data are provided by UNIDATA, and the plume sources, transport, diffusion, and gravitational fallout are considered in the model. The performance of the volcanic ash tracking model PUFF has been examined for Alaskan volcanos (Tanaka et al., 1993; Akasofu and Tanaka, 1993), for Usu volcano (Tanaka and Yamamoto, 2002), and for many actual eruptions occurring in the world, including Sakurajima volcano in Japan. It is the current forecast model of the Alaskan Volcano Observatory.

Recently, Eliasson et al. (2015) have reported the airborne measurement of an ash plume from Sakurajima volcano. By comparing the ash fallout predicted by the PUFF model to that actually measured by the dense observation network around Sakurajima, the discharge rate of ash mass from the crater was estimated by an empirical formula using seismic monitoring and ground deformation data (Iguchi, 2012; 2015). A combination of the real-time PUFF model simulation and the real-time seismicity, tilt and strain monitoring enables the quantitative evaluation of airborne ash density as well as of the distribution of ash fallout on the ground. The prediction system may be applicable to any other volcanoes in the world under the assumption that the relationship derived for Sakurajima is applicable.

The purpose of this study is to simulate, using the PUFF model, the volcanic ash plume dispersal from the February 13, 2014 Kelud volcano. The plume height and emission rate of ash ejected from Kelud volcano are estimated using the empirical formula developed at Sakurajima volcano. In this study, the 3D distributions and temporal variation of airborne ash is estimated quantitatively using the PUFF model. According to the assessment of aviation safety by ICAO, an ash density of 4 mg/m^3 and above is considered to be the danger level for commercial airliners (Kelleher, 2010). The PUFF model simulation is expected to identify the location and spread of the danger zone for the major eruption event of Kelud volcano in Indonesia.

2. Description of the PUFF Model

The PUFF model for real-time volcanic plume prediction was constructed by Tanaka (1994) and reported in detail by Searcy et al. (1998) as an application of pollutant dispersion models (e.g., Praham and Christensen, 1977; Suck et al, 1978; Kai et al, 1988). The model is based on the three-dimensional (3D) Lagrangian form of the Navier-Stokes equations. A transport model can be represented either by an Eulerian or a Lagrangian form. Eularian models solve for variables at fixed locations or grid points: Lagrangian models calculate the trajectories of an ensemble of particles. We assume a vertical column of initial ash particles transported and diffused by winds and turbulence in the 3D space. In the Lagrangian framework, material transport is conducted by the fluid motion, and diffusion is represented by a stochastic process of random walk (e.g., Chatfield, 1984). Here, the plume dispersion model is constructed by a sufficiently large number of random variables $r_i(t)$, $i = 1 \sim M$, representing position vectors of M particles from the origin of the volcanic vent. Gravitational fallout is superimposed on the process of diffusion and transport.

With a discrete time increment Δt, the Lagrangian form of the governing equation may be written as

$$\left\{ \begin{array}{ll} r_i(0) = S, & i = 1 \sim M, \quad \text{for} \quad t = 0, \\ r_i(t+\Delta t) = r_i(t) + V\Delta t + Z\Delta t + G\Delta t, & \\ & i = 1 \sim M, \quad \text{for} \quad t > 0, \end{array} \right. \tag{1}$$

where $r_i = (x, y, z)$ is a position vector of the i-th particle at time t. S designates the initial locations of the particles as a source term. $V = (u, v, w)$ is the local wind velocity to transport the particle, $Z = (c_h, c_h, c_v)$ is a diffusion velocity containing diffusion speeds generated by Gaussian random numbers, and $G = (0, 0, -w_t)$ is the gravitational fallout velocity approximated by extended Stokes Law. Note that the diffusion Z depends on the direction, and the gravity settling G depends on the particle size.

For the computation of the transport, the wind velocity V is obtained from the real-time Grid Point Values (GPV) data provided by the global spectral model (GSM) of the Japan Meteorological Agency (JMA). The GPV data contain weather prediction data from the initial time to 168 hours (7 days) into the future, updated by daily analysis-forecast cycles. The GPV data with 6-hour intervals are first interpolated to the model's time step of 5 minutes using a cubic spline method (see Burden et al., 1981). Then, the wind velocity at an arbitrary spatial point is evaluated using the 3D cubic-splines from the nearby gridded data of 1.25° longitude-latitude intervals and 16 vertical levels from the surface up to 10 hPa. For the real-time PUFF model prediction, the forecast wind data needs to be used. However, for the simulation of a past eruption event, as is the case in this study, the forecast wind data have been replaced by a sequence of initial and forecast data provided by the analysis-forecast cycles. Because the vertical wind speed in GSM is small compared to the fallout speed, the vertical wind is not considered in this study.

The diffusion speed c of the random walk process may be related to the diffusion coefficient K as $c = \sqrt{2K/\Delta t}$, where Δt is set to 5 min in the model. We have repeated diffusion tests with various values of K, and the resulting dispersals are compared to satellite images of actual dispersals from several volcanic eruptions in the past (Tanaka and Yamamoto 2002). With these diffusion tests, we find that the appropriate horizontal diffusion coefficient is $K_h = 150$ (m^2/s). Since the vertical diffusion is considerably smaller than the horizontal diffusion, we set $K_v = 1.5$ (m^2/s) in this study. The vertical diffusion is negligibly small, compared to the gravitational settling. The diffusion coefficients are consistent with in situ observation documented by Eliasson et al. (2015). The default values are used for the first numerical experiment in this study. Then the default values are modified in the second numerical experiment as will be described in the source term.

Gravitational settling is based on an extended Stokes Law for the settling of particles of various grain sizes a. For the volcanic ash, the size may vary widely from fine ash to boulders. According to Khvorostyanov and Curry (2002), the terminal fall speed w_t is approximated by the grain size a and is controlled by a continuous shift from the viscous range to inertial range, as formulated below:

$$\frac{w_t}{w_0} = \frac{a_0}{a}\left[\left\{(\frac{a}{a_0})^3 + \frac{1}{4}\right\}^{\frac{1}{2}} - \frac{1}{2}\right], \quad \ldots\ldots \tag{2}$$

where $a_0 = 150$ μm is the particle size separating the viscous range and inertial range. The parameter w_0= 1.0 m/s

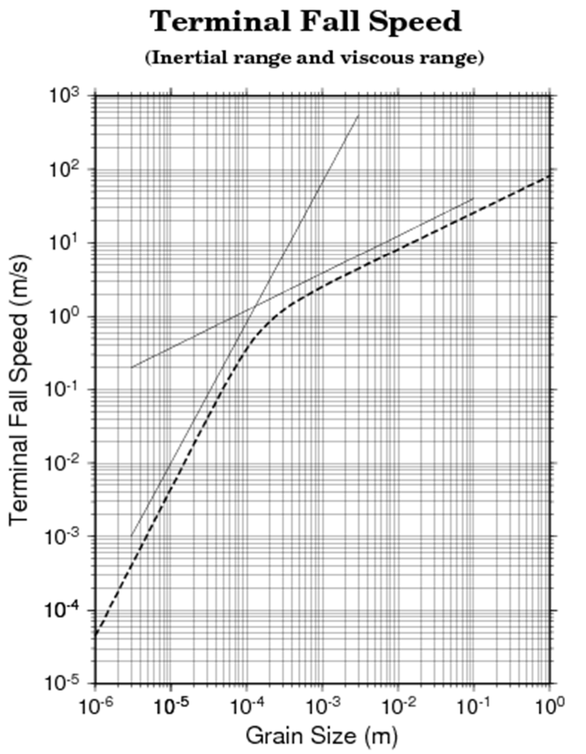

Fig. 2. Terminal fall speed (m/s) as a function of particle diameter (m). Small particles obey the 2 power law of grain size, and large particles obey the $1/2$ power of grain size. The two slopes are separated by the Stokes law limit.

is the terminal fall speed characterized by a_0. **Fig. 2** shows the terminal fall speed w_t as a function of the grain size a over the range from 1 μm to 1 m. For particles larger than a_0, the fall speed is controlled by the inertial resistance with the power 1/2 exceeding w_0, whereas for particles smaller than a_0, the fallout speed decreases from w_0, controlled by the viscosity with the power 2. The fallout speed in this study is quite similar to the terminal fall speed documented by Fig. 1 of Folch (2012). The boundary of the two regimes is referred to as the Stokes law limit.

Actual eruptions contain from large fragments of up to a few meters in diameter to fine ash with particle sizes under 1 μm. Large particles settle out within a short time, and the particle size spectrum in the ash plume tends to decrease in scale. Because we are interested in the particles that can travel for several hours, we have assumed an initial particle size of logarithmic Gaussian distribution with its standard deviation 1.0 centered at -4.5 on a log scale, meaning a particle size of 32 μm. The gravitational settling in the PUFF model was examined in Searcy et al. (1998, see their Fig. 3) for various particle size distributions. The results demonstrate that particles greater than about 10^{-4} m fall out within the first few time steps, and the remaining particles stay in the air for several hours. There have been a number of studies done on the total grain size distribution, e.g., by Macedonio et al. (1988), Woods and Bursik (1991), and Rust and Cashmann (2011). Refer to these studies for details and a mathematical description of grain size distributions.

Modeling the source S of the eruption, the number of particles released at every time step may be adjusted in order to draw optimal statistical information from the model products. In this study, we generate a maximum of $M_0 = 5000$ particles uniformly in time using a uniform random number generator over the time step Δt, which scales the emission rate. Although it is possible to increase the number toward the limit of computer capability, we avoid excessive complication and sophistication for the application of an urgent operational prediction with restricted available information. **Table 1** lists the time change of the emission rate (10^6 ton/hour) and plume height (km) as the input for the PUFF model, estimated by the seismicity, tilt and strain record near the Kelud volcano (see Iguchi 2015). The plume height z_2 reached 17.1 km, and the emission rate ε was 21.7×10^6 ton/hour during the first hour. Based on the maximum number of M_0 assigned for this maximum emission rate ε, we find that one particle contains 360 tons of ash mass. The number of source particles M_0 for one time step decreases with time scaled linearly with the emission rate ε.

Given an initial vertical velocity of the emission with a specified damping (e-folding) time τ, the particles generated by a uniform random number in time are redistributed in the vertical from the vent z_1 to the plume top level z_2. Using time integration for the vertical velocity and elimination of the initial velocity, the final form is given as $z(t) = z_2 - (z_2 - z_1)\exp(-t/\tau)$ during the time step Δt. Since z_1 and z_2 are given, we can put a large number of particles near the plume top by adjusting the damping time τ, which is set to 30 s in this study. The resulting ash distribution (see **Fig. 7**) contains more particles near the plume top, as shown by exponential form in Fig. 2 by Searcy et al. (1998). Therefore, the source $S = (x, y, z)$ contains the 3D location of an initial particle with an additional property being the particle size a.

Compared to the satellite observation in **Fig. 1**, it has been found that the diffusion speed estimated by previous studies appears to be too small for the Kelud volcano eruption used in the present study (see **Figs. 4** and **5**). The upward mass flux converges near the plume top and then diverges horizontally, indicating a considerable amount of diverging mass flux around the volcano. The diffusion coefficient is thus amplified in the vertical direction by a linear scaling around the volcano. The amplified diffusion coefficient is reduced in the horizontal direction by the Gaussian function scaled by a radius from the vent as

$$c'_h = c_h \times \left[1 + \frac{z}{z_0} exp \left\{ - \left(\frac{r}{r_0} \right)^2 \right\} \right]. \quad \quad . \; . \quad (3)$$

We set z_0 = 330 m and $r_0 = 300$ km in this study by adjusting the initial ash dispersion to match the satellite imagery. The large diffusion near the volcano represents the initial momentum of the mass flux diverging from the vertical column over the volcano. The large diffusion converges to the default values at the great distance. In this

Table 1. Time change of the emission rate ε (10^6 ton/hour), number of particles released for one time step M_0, and plume height z_2 (km). Both local time and UTC are specified.

Local time	Emission rate	M_0	Plume height	UTC
2014 2 13 23 00	21.7	5000	17.056	2014 2 13 16 00
2014 2 14 00 00	14.1	3248	15.321	2014 2 13 17 00
2014 2 14 01 00	9.39	2163	13.839	2014 2 13 18 00
2014 2 14 02 00	6.37	1467	12.562	2014 2 13 19 00
2014 2 14 03 00	4.41	1016	11.453	2014 2 13 20 00
2014 2 14 04 00	3.09	711	10.486	2014 2 13 21 00
2014 2 14 05 00	2.21	509	9.636	2014 2 13 22 00
2014 2 14 06 00	1.60	368	8.885	2014 2 13 23 00
2014 2 14 07 00	1.17	269	8.219	2014 2 14 00 00
2014 2 14 08 00	0.865	199	7.625	2014 2 14 01 00
2014 2 14 09 00	0.648	149	7.093	2014 2 14 02 00

study, the default values are used for the first numerical experiment. The default values are then modified in the second numerical experiment in reference to the satellite imagery analyzed after the eruption.

The governing model equation is integrated in time, and the distribution of the particles in the atmosphere is presented in various mapping projections. The total number of the plume particles M in the atmosphere increases with each time step. When the particles drop to the ground, the fallout locations are recorded. Likewise, when the particles have moved out from the prescribed computing domain, they are removed from the computation. The distribution of total ash fallout is computed by counting the total number and total mass of the ash particles in a unit area on the ground. Likewise, the distribution of the airborne ash density is computed by counting the total number and total mass of the ash particles in a unit volume in the atmosphere. The output products of the map projections are drafted using the Generic Mapping Tools software (Wessel et al. 2013) and are open to the public through the SATREPS Web Site.

3. Result of the Model Simulation

The performance of the PUFF model simulation of the ash dispersal relies totally on the accuracy of the wind data provided by JMA/GSM. The output data from GSM with 1.25° longitude-latitude grids are coarser than the meso-scale numerical weather prediction models. However, they have the advantage of covering the entire world so that the PUFF model is applicable to any volcanic eruption in the world, although the parameters in the model may need further calibrations.

Figure 3 illustrates the distribution of geopotential height and wind vector at 100 hPa and 700 hPa levels at 18:00 UTC on February 13, 2014 (1:00 am local time). The real-time GPV data are provided by the Japan Meteorological Agency through the portal site at the Center for Computational Sciences of the University of Tsukuba. The 100 hPa map shows that strong easterly winds blew at 25 m/s over Java at an altitude of about 16.5 km. In contrast, the 700 hPa map shows a southwesterly flow of 9 m/s over Kelud volcano.

Figure 4 illustrates the results of the PUFF model simulation of the ash plume dispersal 1, 3, 5, and 7 hours after the initial eruption that started at 16:00 UTC. The colors indicate different plume heights. For the first experiment, we used the default parameters of the particle source at the vertical column over the vent and a uniform diffusion coefficient, as used in Tanaka and Yamamoto (2002). The result for 1 hour after the onset of the eruption shows a point source of the plume due to the small amount of diffusion. Three hours after the onset of the eruption, the ash plume starts to drift westward with the strong easterly flow at an altitude of 17 km. The result for 5 hours after the eruption shows further westward drift with the plume top (red) reaching Yogyakarta. Plume height decreases at the source region. Interestingly, the lower part of the plume (blue) moves northeast, reaching Surabaya. The result for 7 hours after onset shows the plume top (red) reaching 107° E. The shape and extension of the ash plume is somewhat different from that in the satellite observation in **Fig. 1**.

Figure 5 depicts zonal-height (X-Z) and meridional-height (Y-Z) cross sections of ash plume dispersal for every hour starting from the onset of the eruption. The plume shape for the first hour is a simple vertical column over the vent. The result of the X-Z section shows a westward movement of airborne ash caused by winds at high altitude. The plume height gradually decreases over the vent with time, and the area of high concentration tilts westward with respect to height. The result of the Y-Z section shows that the upper level plume moves northward, and the middle level plume moves southward. Then, the lower level plume moves northward again, indicating a complicated vertical wind shear in the meridional wind. It is clear that the initial plume has an umbrella shape according to the satellite imagery, and the simple vertical column of ash is insufficient to represent the observed ash dispersal.

The same PUFF model simulation was conducted with an improved formula for the particle source and locally enhanced diffusion coefficient described in section 2 of

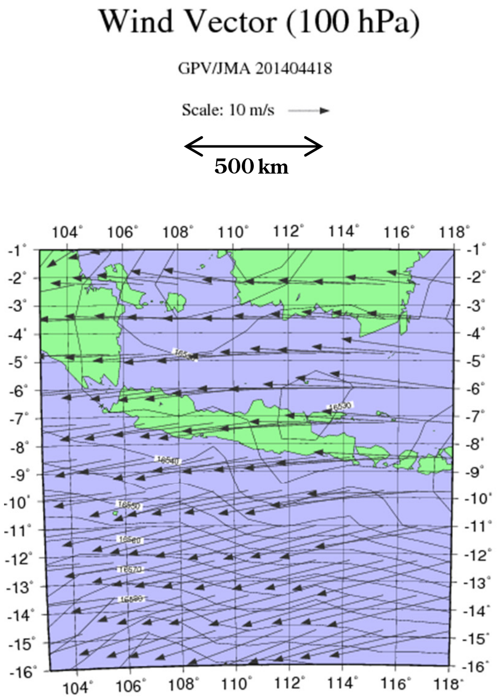

Fig. 3. Distribution of geopotential height and wind vector at 100 hPa and 700 hPa levels at 18:00 UTC on February 13, 2014 (1:00 am local time). The real-time GPV data is provided by Japan Meteorological Agency through the Center for Computational Science, University of Tsukuba.

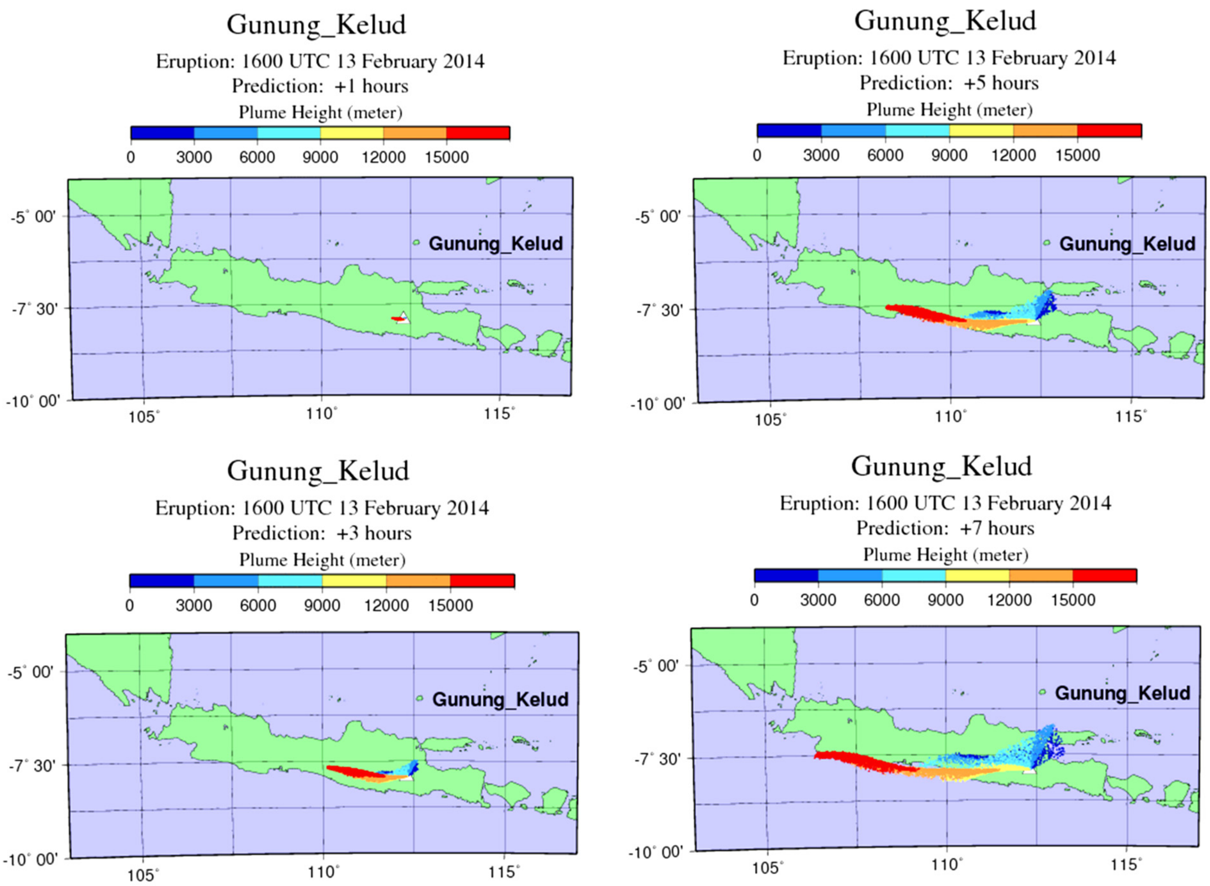

Fig. 4. PUFF model simulations of the ash plume dispersal for 1, 3, 5, and 7 hours after the onset of the eruption at 16:00 UTC. The particle colors indicate different plume heights. Default parameters are used for particle source and diffusion. For plotting purposes the particle number is reduced to 1/10.

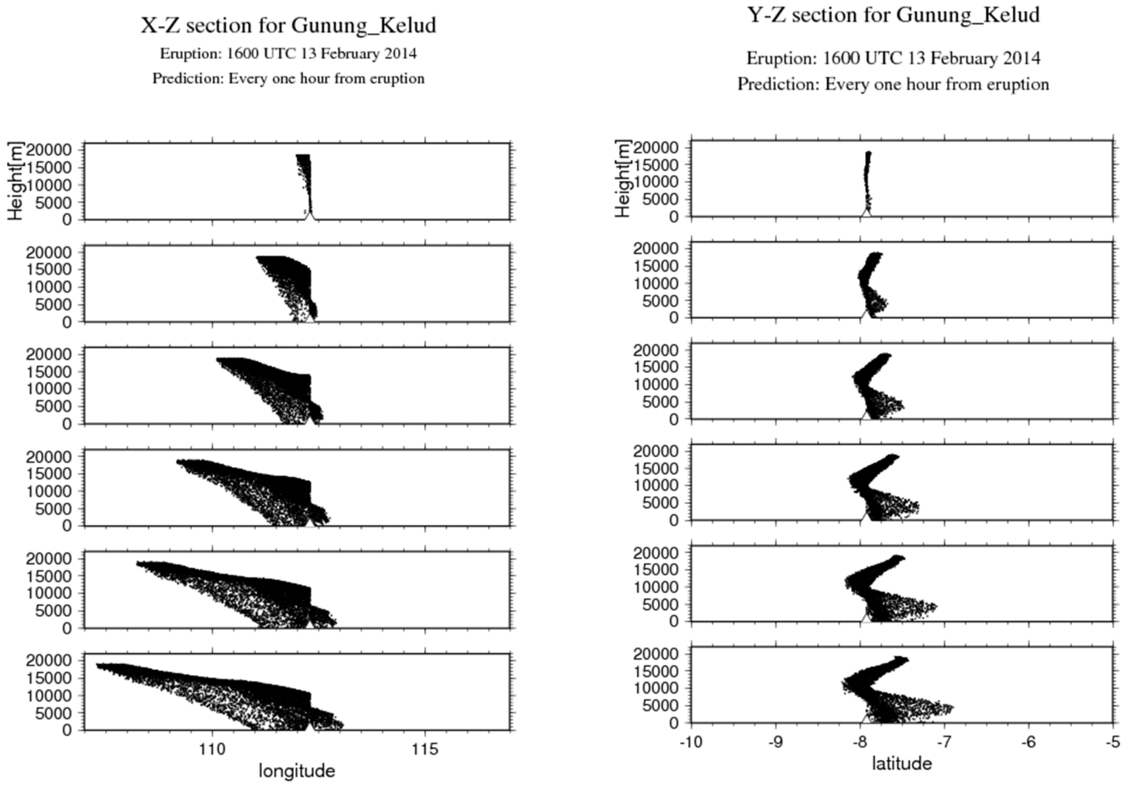

Fig. 5. Ash plume dispersal in zonal-height (X-Z) and meridional-height (Y-Z) cross sections for each hour from the onset of the eruption at 16:00 UTC. Default parameters are used for particle source and diffusion.

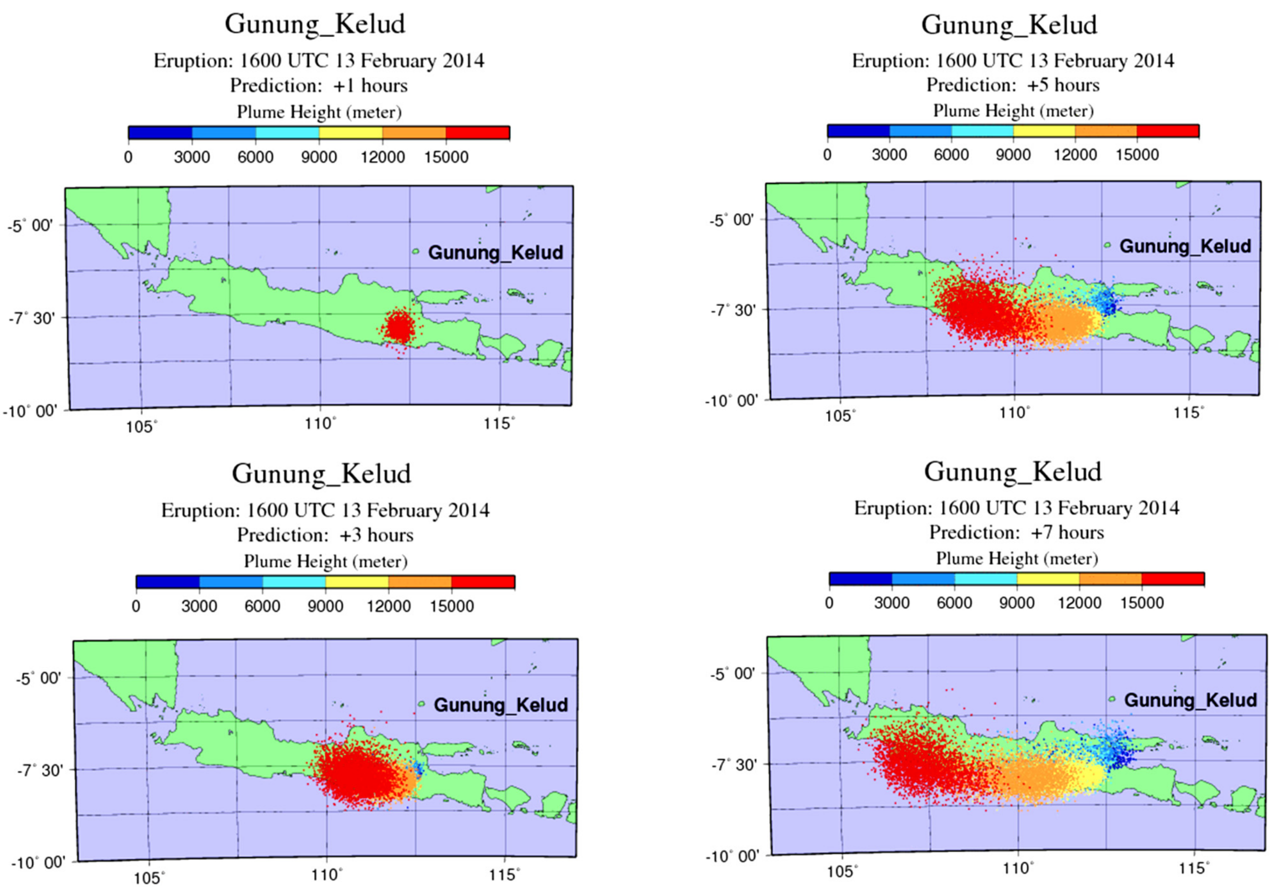

Fig. 6. PUFF model simulations of the ash plume dispersal for 1, 3, 5, and 7 hours after the onset of the eruption at 16:00 UTC. The particle colors indicate plume heights. Improved parameters are used for particle source and diffusion. For plotting purposes the particle number is reduced to 1/10.

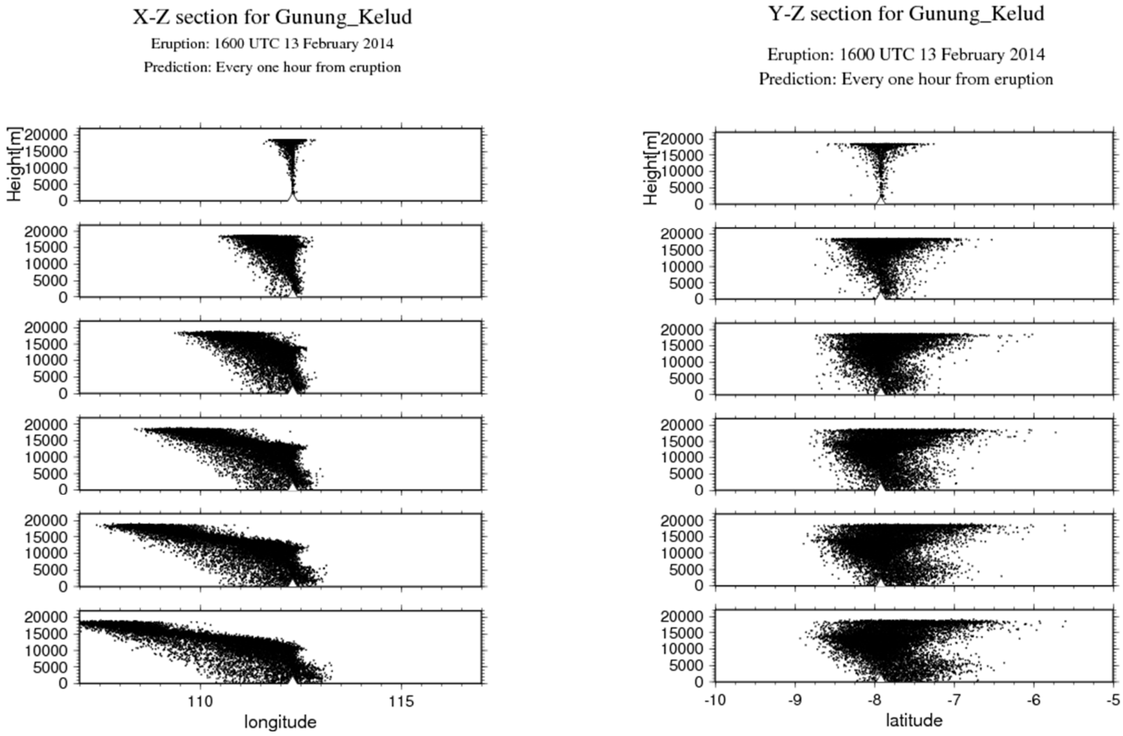

Fig. 7. Ash plume dispersal in zonal-height (X-Z) and meridional-height (Y-Z) cross sections for each hour from the onset of the eruption at 16:00 UTC. Improved parameters are used for particle source and diffusion.

this study. **Fig. 6** illustrates the results of the improved model simulation of the ash plume dispersal 1, 3, 5, and 7 hours into the eruption that started at 16:00 UTC. The result for 1 hour after the onset of the eruption shows a plume top rounded by the enhanced diffusion. The extension of the circular plume agrees with the satellite images in **Fig. 1**. Three hours after the onset of the eruption, the ash plume starts to drift westward, carried by the strong easterly flow at the altitude of 17 km. The result after 5 hours shows further westward drift with the plume top (red) reaching Yogyakarta. Plume height decreases at the source. The lower part of the plume (blue) moves northeast, reaching Surabaya. The result for 7 hours after the onset of the eruption shows the plume top (red) between 106 and 110° E, as is consistent with the satellite imagery in **Fig. 1**. The location shifts slightly northward in the model simulation. This may be caused by a difference in direction between actual winds and those in the model. Part of the plume clearly moves to northeast from the vent as shown by the low level particles (blue).

Figure 7 illustrates zonal-height (X-Z) and meridional-height (Y-Z) cross sections of ash plume dispersal for every hour, starting from the onset of the eruption with improved parameters. The plume for the first hour has an anvil shape with a large spread at the plume top in both in X-Z and Y-Z sections. The result of the X-Z section shows a flat plume top extending westward, pushed by winds at high altitude. A minor counter flow is seen at the top level, caused by the large diverging flow near the volcano. There are many particles settling out of the anvil plume on the west side of the volcano. The plume height gradually decreases with time over the vent, and the area of high concentration tilts westward with respect to height. The result of the Y-Z section shows a clear anvil shape extending north and south from the volcano forming an umbrella-shape of the ash plume. The upper-level plume extends northward, and the mid-level plume extends southward. The lower level plume extends northward again, indicating a complicated vertical wind shear in the meridional wind.

Figure 8 (left) shows the particle distribution for ash fallout that accumulated over the course of 56 hours from the start of the eruption. The fallout covers almost the entire island of Java, including Bandung and Solo in the west. It also covers Surabaya to the northeast. Interestingly, there is no ash fallout east of the volcano. Because one particle contains 360 tons of ash mass, we can estimate the concentration of ash fallout in units of g/m^2. **Fig. 8 (right)** shows the contours of the ash fallout in common log-scale, i.e., 2 denotes 100 g/m^2. The 1000 g/m^2 contour extends 70 km to the west of the volcano. The 250 g/m^2 contour reaches Surabaya while the 200 g/m^2 contour extends up to Yogyakarta. The result seems to be less than that in the actual fallout reports. The discrepancy may be caused by the grain size distribution with the mean size of 32 μm. If the mean size is set much larger, the result would show more fallout near the volcano. Since the current model is adjusted for aviation purposes, such an attempt is beyond the scope of this study.

Figure 9 gives a 3D perspective of the volcanic ash plume dispersal from Kelud volcano at 23:00 UTC on

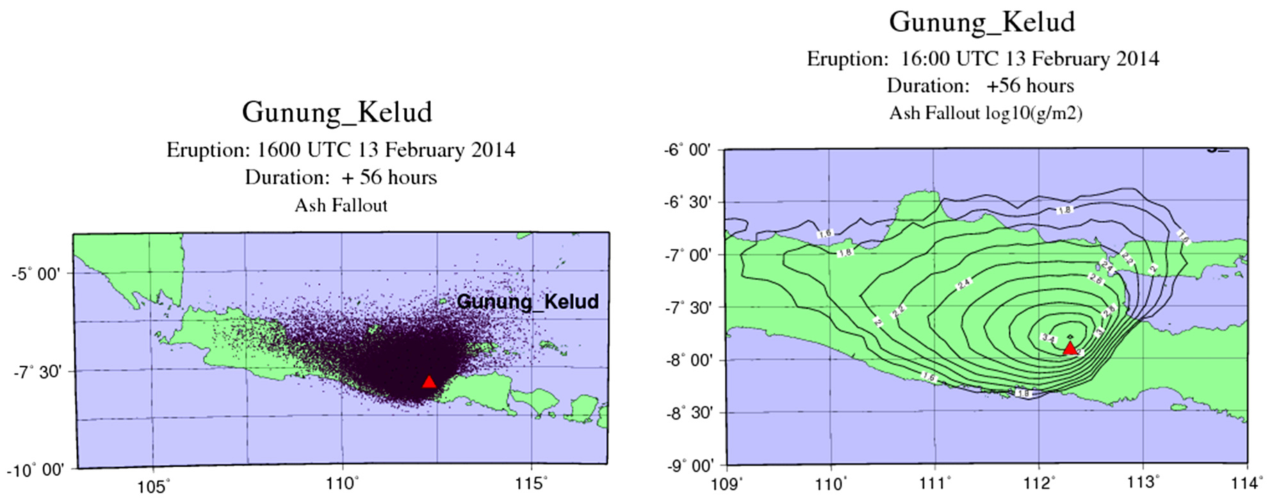

Fig. 8. Particle distribution of ash fallout over 56 hours from the onset of the eruption (left), and the estimated concentration of ash fallout (g/m^2) in common log-scale, i.e., 2 denotes 100 g/m^2 (right).

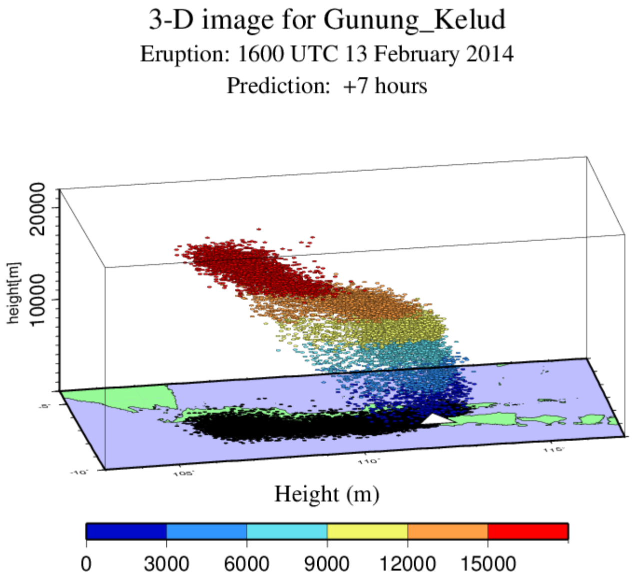

Fig. 9. The 3D perspective of the volcanic ash plume dispersal from Kelud volcano at 23:00 UTC on February 13, 2014. The particle colors indicate different plume heights, and the projection onto the ground is marked by black dots. For plotting purposes the particle number is reduced to 1/10.

February 13, 2014. The figure is for 7 hours after the onset of the eruption. The colors of particles indicate different plume heights, and the projection onto the ground is marked by black dots. Since the plume top reaches 17 km, strong easterly winds transport the ash plume westward, tilting it in that direction. The figure shows fallout of large particles from the anvil ash cloud.

Finally, **Fig. 10** shows the distribution of airborne ash density (mg/m^3) for 1, 3, 5, and 7 hours after the onset of the eruption. The values are in common log-scale, i.e., 2 denotes 100 mg/m^3. In the result, the values of the highest density in the vertical column are projected onto the ground. For the result 1 hour after the onset of the eruption, the circular shape of the ash plume is clearly identifiable. In the core region, there is a contour of 1000 mg/m^3 within 50 km from the volcano. The outer contour, labeled 1, represents an ash density of 10 mg/m^3. This area is clearly recognized as an aviation danger zone. For the result 3 hours after the eruption, the core area with 1000 mg/m^3 is unchanged located within 50 km west of the volcano. The area with 100 mg/m^3 extends 300 km to the west of the volcano and covers Yogyakarta Airport. Surabaya Airport to the northeast is also covered by the area with 100 mg/m^3. The area of ash density with 10 mg/m^3 is close to the area with 100 mg/m^3. The result suggests that the ash density changes abruptly from the safe zone to the danger zone at the edge of the airborne ash plume. After 5 hours, the contour of 1000 mg/m^3 almost disappears. The area with 100 mg/m^3 occupies most of the island of Java, except for the western and eastern edges of the island. The area with 10 mg/m^3 appears slightly outside the contour of 100 mg/m^3. Finally, 7 hours after the eruption, the area with 10 mg/m^3 covers almost all of Java, except for its eastern edge. The result suggests that even the Soekarno-Hatta International Airport in Jakarta is inside the danger zone for commercial airliners, as the level exceeds 10 mg/m^3. Although the satellite images in **Fig. 1** show the location of the ash plume to be only in the southern half of western Java, the simulation results indicate a rather wide area of the danger zone. The airborne ash density simulated by the PUFF model provides quantitative information about the possible extension of the danger zone for the eruption event of Kelud volcano in February 2014.

4. Conclusion

A major Plinian eruption occurred at Kelud volcano at 15:50 UTC on February 13, 2014. The ash plume reached well into the stratosphere at 17 km above the ground. According to GMS satellite monitoring, the plume top spread to take on an anvil shape around the volcano. The initial explosive momentum of the eruption extended the radius

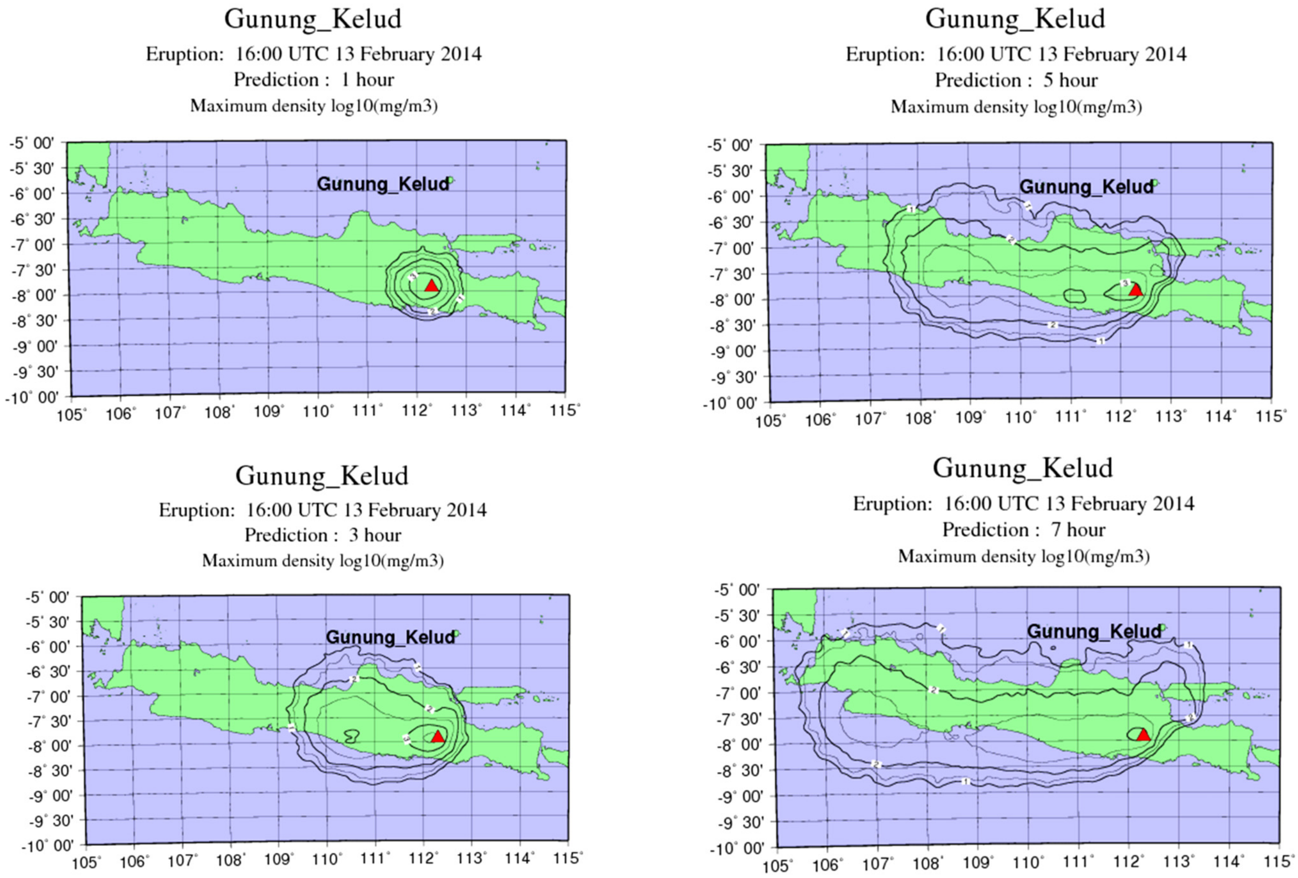

Fig. 10. Distribution of airborne ash density (mg/m^3) 1, 3, 5, and 7 hours after the onset of the eruption. The values are in common log-scale, i.e., 2 denotes 100 mg/m^3.

of the ash cloud to 200 km within the first two hours. The circular shape of the plume top drifted westward across Java, gradually spreading due to diffusive mixing. By 9 hours after the initial eruption, the center of the plume top had drifted 600 km westward.

In this study, the sequence of airborne ash dispersal from Kelud volcano was simulated using the PUFF model. The emission rate of ash mass from the vent was estimated from the empirical formulae tested at Sakurajima volcano using seismic monitoring data (Iguchi, 2015). In this study, the 3D distributions and extension of ash density was estimated quantitatively using the PUFF model. According to ICAO, an ash density of 4 mg/m^3 and above is considered dangerous for commercial airliners.

According to the result of the PUFF model simulation, the circular shape of the anvil ash cloud at 17 km height had extended for the first two hours over a radius of 200 km from Kelud volcano. The core region within 50 km of the volcano showed an airborne ash density of 1000 mg/m^3. The density dropped to 10 mg/m^3 at the edge of the anvil ash plume at 200 km from the volcano. It was demonstrated that a simple vertical column of initial particle source was insufficient to represent the major Plinian eruption. Three hours after the onset of the eruption, the area with 100 mg/m^3 extended 300 km west of the volcano, covering Yogyakarta Airport. Due to the low level wind, Surabaya Airport to the northeast was also covered by the area with 100 mg/m^3. The result of the ash plume dispersal 7 hours after the onset of the eruption indicated that almost of the entire island of Java was covered by the danger zone for commercial airliners, as ash exceeded 10 mg/m^3. Although the satellite images showed the location of ash plume to be only in the southern half of western Java, the simulation results quantitatively indicated the wider danger zone for aircraft.

The horizontal distribution of ash fallout was estimated using the model simulation. The results indicate 250 g/m^2 of ash fallout at Surabaya, and 200 g/m^2 at Yogyakarta. These results are substantially smaller than the amount stated in the actual fallout reports. The discrepancy may have been caused by the grain size distribution centered at 32 μm. Further improvement is needed for the PUFF model simulation to correlate well with ground observations.

Acknowledgements

The authors are grateful to Dr. Junichi Yoshitani of Kyoto University and Dr. Makoto Shimomura of the University of Tsukuba for their meaningful comments. The authors also appreciate the technical assistance rendered by Dr. Dodo Gunawan of BMKG and Mr. Mamoru Izumi. This research was supported by the SATREPS research project.

References:

[1] S.-I. Akasofu, and H. L. Tanaka, "Urgent issue of developing volcanic ash tracking model," Kagaku Asahi, No.5, pp. 121-124, 1993 (in Japanese).

[2] P. Armienti, and G. Macedonio, "A numerical model for simulation of tephra transport and deposition: Application to May 18, 1980, Mount St. Helens eruption," J. Geophys. Res., Vol.93, pp. 6463-6476, 1988.

[3] R. L. Burden, J. D. Faires, and A. C. Reynolds, "Numerical analysis," Prindle, Weber and Schmidt, 598pp., 1981.

[4] T. L. Casadevall, "The 1989-1990 eruption of Redoubt volcano, Alaska: Impacts on aircraft operations," J. Volcanol. Geotherm. Res., Vol.62, pp. 301-316, 1994.

[5] C. Chatfield, "The analysis of time series: An introduction," Chapman and Hall, 286pp., 1984.

[6] K. G. Dean, S. I. Akasofu, and H. L. Tanaka, "Volcanic hazards and aviation safety: Developing techniques in Alaska," FAA Aviation Safety Journal, Vol.3, No.1, pp. 11-15, 1993.

[7] I. Eliasson, J. Yoshitani, K. Weher, N. Yasuda, M. Iguchi, and A. Vogel, "Airborne measurement in the ash plume from Mount Sakurajima: Analysis of gravitational effect on dispersion and fallout," Intl. J. Atmos. Sci., Vol.2014, Article ID372135, 16p., 2015.

[8] A. Folch, "A review of tephra transport and dispersal models: Evolution, current status, and future perspectives," Journal of Volcanology and Geothermal Research, Vol.235-236, pp. 96-115, 2012.

[9] L. S. Glaze, and S. Self, "Ashfall dispersal for the 16 September 1986, eruption of Lascar, Chile, calculated by a turbulent diffusion model," Geophys. Res. Let., Vol.18, pp. 1237-1240, 1991.

[10] J. L. Heffter, and B. J. B. Stunder, "Volcanic ash forecast transport and dispersion (VAFTAD) model," Computer Techniques, Vol.8, pp. 533-541, 1993.

[11] P. V. Hobbs, L. F. Radke, J. H. Lyons, R. J. Ferek, D. J. Coffman, and T. J. Casadevall, "Airborne measurements of particle and gas emissions from the 1990 volcanic eruption of Mount Redoubt," J. Geophys. Res. Vol.96, pp. 18735-18752, 1991.

[12] A. W. Hurst, and R. Turner, "Performance of the program ASHFALL for forecasting ash fall during the 1995 and 1996 eruptions of Ruapehu volcano, New Zealand," J. Geol. and Geophys., Vol.42, pp. 615-622, 1999.

[13] M. Iguchi, "Prediction of volume of volcanic ash ejected from Showa crater of Sakurajima volcano, Japan," Disaster Prevention Research Institute, Annual Report B, University of Kyoto, Vol.55, pp. 169-175, 2012.

[14] M. Iguchi, "A method for real-time evaluation of discharge rate of volcanic ash: Case study on intermittent eruptions at the Sakurajima volcano, Japan," 2015 (submitted to JDR).

[15] K. Kai, Y. Okada, O. Uchino, I. Tabata, H. Nakamura, T. Takasugi, and Y. Nikaidou, "Lidar observation and numerical simulation of Kosa (Asian Dust) over Tsukuba, Japan, during the spring of 1986," J. Meteor. Soc. Japan, Vol.66, pp. 457-472, 1988.

[16] R. Kelleher, "Atlantic conference on Eyjafjallajokull and aviation," UK volcanic ash safety regulation, Keflavic Airport, Iceland, 2010.

[17] V. Khvorostyanov, and J. A. Curry, "Terminal velocities of droplets and crystals: Power laws with continuous parameters over the size spectrum," J. Atmos. Sci., Vol.59, pp. 1872-1884, 2002.

[18] J. Kienle, A. W. Woods, S. A. Estes, K. Ahlnaes, K. G. Dean, and H. L. Tanaka, "Satellite and slow-scan television observations of the rise and dispersion of ash-rich eruption clouds from Redoubt volcano, Alaska," EOS, Vol. 72, No.2, pp. 748-750, 1991.

[19] S. Leadbetter, P. Agnew, L. Burgin, et al., "Overview of the NAME model and its role as a VAAC atmospheric dispersion model during the Eyjafjallajokull eruption April 2010," Proc. EGU General Assembly, Vienna, Austria, p. 15765, 2010.

[20] G. Macedonio, M. T. Parecshi, and R. Santacroce, "A numerical simulation of the Plinian fall phase of 79 A.D. eruption of Vesuvius," J. Geophys. Res. Vol.93, No.B12, pp. 14817-14827, 1988.

[21] S. Onodera, "Volcanic activity and flight operations," Aviation Meteorological Notes, Vol.45, pp. 13-30, 1997.

[22] S. Onodera, "A study on the prevention of aircraft encounter with volcanic ash in proximity area between airways and active volcano," Dissertation for Ph. D., Life and Environmental Sciences, University of Tsukuba, 272pp., 2013.

[23] L. P. Praham, and O. Christensen, "Long-range transmission of pollutant simulated by a two-dimensional pseudo spectral dispersion model," J. Appl. Meteor., Vol.16, pp. 896-910, 1977.

[24] A. J. Prata, "Satellite detection of hazardous volcanic clouds and the risk to global air traffic," Nat Hazards, Vol.51, pp. 303-324, 2009.

[25] A. C. Rust, and K. V. Cashman, "Permeability controls on expansion and size distributions of pyroclasts," J. Geophys. Res., Solid Earth, 1978-2012, 116. B11, 2011.

[26] C. Searcy, K. Dean, and B. Stringer, "PUFF: A volcanic ash tracking and prediction model," J. Volc. and Geophys. Res., Vol.80, Nos.1-2, pp. 1-16, 1998.

[27] S. H. Suck, E. C. Upchurch, and J. R. Brock, "Dust transport in Maricopa county, Arizona," Atmos. Environ, Vol.12, pp. 2265-2271, 1978.

[28] H. L. Tanaka, "Development of a prediction scheme for the volcanic ash fall from Redoubt volcano," First Int'l. Symp. on Volcanic Ash and Aviation Safety, Seattle, Washington. U.S. Geological Survey, Circular 1065, 58, 1991.

[29] H. L. Tanaka, K. G. Dean, and S. I. Akasofu, "Predicting the movement of volcanic ash clouds," EOS, Vol.74, No.20, pp. 231-231, 1993.

[30] H. L. Tanaka, "Development of a prediction scheme for volcanic ash fall from Redoubt volcano, Alaska," Proc. First International Symposium on Volcanic Ash and Aviation Safety, U.S. Geological Survey, Bulletin 2047, pp. 283-291, 1994.

[31] H.L. Tanaka, and K. Yamamoto, "Numerical simulations of volcanic plume dispersal from Usu volcano in Japan on 31 March 2000," Earth, Planets and Space, Vol.54, pp. 743-752, 2002.

[32] Tokyo Aviation Weather Service Center, "Volcanic ash advisory service, Japan Meteorological Agency," Geophys. Maga. Ser. 2, Vol.4, Nos.1-4, 2001.

[33] H. E. Thomas, and I. M. Watson, "Observations of volcanic emissions from space: current and future perspectives," Nat. Hazards, Vol.54, pp. 323-354, 2010.

[34] P. Wessel, W. H. F. Smith, R. Scharroo, J. F. Luis, and F. Wobbe, "Generic Mapping Tools: Improved version released," EOS Trans, AGU, Vol.94, pp. 409-410, 2013.

[35] A. W. Woods, and M. I. Bursik, "Particle fallout, thermal disequilibrium and volcanic plumes," Bulletin of Volcanology, Vol.53, No.7, pp. 559-570, 1991.

Name:
Hiroshi L. Tanaka

Affiliation:
Center for Computational Sciences, Division of Geoenvironmental Science, University of Tsukuba

Address:
Tsukuba, 305-8577, Japan

Brief Career:

1981-1988 Sr. Research Specialist, Atmospheric Sciences, University of Missouri-Columbia, USA
1988-1991 Assistant Professor, Geophysical Institute, University of Alaska Fairbanks, USA
1991-2001 Assistant Professor, Institute of Geoscience, University of Tsukuba, Japan
2001-2005 Associate Professor, Life and Environmental Science, University of Tsukuba, Japan
2005-present Full Professor, Center for Computational Sciences, University of Tsukuba, Japan

Selected Publications:

- H. L. Tanaka and K. Yamamoto, "Numerical simulations of volcanic plume dispersal from Usu volcano in Japan on 31 March 2000," Earth, Planets and Space, Vol.54, pp. 743-752, 2002.
- H. L. Tanaka, K.G. Dean, and S.I. Akasofu, "Predicting the movement of volcanic ash clouds," EOS, Vol.74, No.20, pp. 231-231, 1993.
- K. G. Dean, S.I. Akasofu, and H. L. Tanaka, "Volcanic hazards and aviation safety: Developing techniques in Alaska," FAA Aviation Safety Journal, Vol.3, No.1, pp. 11-15, 1993.

Academic Societies & Scientific Organizations:

- Metrological Society of Japan (MSJ)
- American Geophysical Union (AGU)

Name:
Masato Iguchi

Affiliation:
Professor, Disaster Prevention Research Institute, Kyoto University

Address:
1722-19 Sakurajima-Yokoyama, Kagoshima 891-1419, Japan

Brief Career:
1981- Research Associate, DPRI
1995- Associate Professor, DPRI
2012- Professor, DPRI

Selected Publications:
• "Magma movement from the deep to shallow Sakurajima volcano as revealed by geophysical observations," Bull. Volcanol. Soc. Japan, Vol.58, pp. 1-18, 2013.
• "Volcanic Earthquakes and Tremors in Japan," Kyoto University Press, p. 253, 2011.

Academic Societies & Scientific Organizations:
• Volcanological Society of Japan (VSJ)
• American Geophysical Union (AGU)

Name:
Setsuya Nakada

Affiliation:
Professor, Earthquake Research Institute, The University of Tokyo

Address:
1-1-1 Yayoi, Bunkyo-ku, Tokyo 113-0032, Japan

Brief Career:
1979 Research Associate, Kyushu University
1995 Associate Professor, Earthquake Research Institute, The University of Tokyo
1999 Professor, Earthquake Research Institute, The University of Tokyo

Selected Publications:
• "Miocene-Holocene volcanism," The Geology of Japan (Moreno, T. et al., Eds.), Geological Society of London, pp. 273-308, 2016.
• "The outline of the 2011 eruption at Shinmoe-dake (Kirishima), Japan," Earth Planets Space, Vol.65, pp. 475-488, 2013.

Academic Societies & Scientific Organizations:
• International Association of Volcanology and Chemistry of the Earth's Interior (IAVCEI)
• American Geophysical Union (AGU)
• Volcanological Society of Japan (VSJ)